Characterization of TCO/p contact resistance in a-Si:H p-i-n solar cells under illumination

R. KAPLAN*, B. KAPLAN
Department of Secondary Science and Mathematics Education, University of Mersin, Yenisehir Campus, 33169 Mersin, Turkey

A different method is given to measure the transparent-conductive-oxide/p-layer (TCO/p) contact and the TCO sheet resistance in a-Si:H based p-i-n superstrate solar cells under light. The method first needs having scribed TCO strips, which are electrically isolated before a-Si:H deposition, and then fabricating rows of individual devices on each strip. Analysis of 4-probe measurements in different V-sensing designs straighly gives the TCO/p contact and TCO sheet resistance. We applied this method to solar cell devices deposited on commercial SnO_2 substrates. The TCO/p contact resistance is determined to be ~0.2 Ω-cm^2 and the sheet resistance 2.9 Ω/sq under illumination. These values are smaller than those of dark results as compared, and thus they make a negligible contribution to the total series resistance of the solar cell devices.

(Received October 22, 2013; accepted September 11, 2014)

Keywords: Amorphous Si solar cells, J-V characterization, TCO/p contact-resistance, Sheet-resistance

1. Introduction

Hydrogenated amorphous silicon (a-Si:H) based p-i-n solar cells have been investigated extensively due to their significant cost reduction, large scale deposition and better efficiency [1]. Unlike crystalline silicon, a-Si:H is comparatively broader band gap material in which p-layer minimizes the absorption losses due to the fact that photons below band gap energy can be transmitted to i-layer. The band gap of a-Si:H (1.8 eV) is still low and it leads to sufficient absorption losses, while employing it as a p-layer [2].

One focus of today's research is the optimization of the transparent conductive electrodes to obtain higher efficiencies [3-10]. An integral part of the solar cells are the transparent conductive oxide (TCO) layers used as a front electrode. When applied as the front side, TCO has to posses a high transparency in the spectral region where the solar cell is operating and a high electrical conductivity. In addition, TCO plays an important role in the light trapping [11] and a large effort is devoted to improving the optical, electrical and surface properties of the TCO materials, such as tin oxide (SnO_2), indium-tin oxide (ITO), and zinc oxide (ZnO). The TCO surface influences the electrical properties of the solar cell, as it determines the interface area and chemistry of the TCO/Si-p-layer interface. One major challenge in producing high quality SnO_2 is the fact that usually surface roughness (and hence light scattering) and thickness are correlated. Often a certain minimum thickness is required to develop a surface of sufficent feature size and roughness, leading to an increased absorption of the TCO.

In general, the sheet resistance R_{sh} of high quality TCO shuld be not larger than about 10 Ω and the average absorption of TCO on highly transparent glass $A_{400-1100}$ between 400 and 1100 nm should be below about 6-7 % [12]. Such absorption values from optical transmission and reflection data are best measured with index matching fluid to avoid errors due to the surface roughness of the TCO. However, the minimum requirements for the optical and electrical properties of the TCO depend on the structure and the absorber material of the solar cell. For a-Si:H absorber layers a high transparency for visible light (wavelength λ=400-750 nm) is sufficient.

For superstrate a-Si:H TCO/p-i-n solar cells, minimizing the resistance between the p-layer and TCO is a critical issue for the incorporation of new TCO materials like ZnO or alloys of Zn-In-O and Zn-Sn-O and new p-layers like μc-SiC or μc-SiO into devices [13]. However, characterization of the TCO/p interface is difficult since it is in series with the dominant p-i-n junction.

We present a method [14-16] to characterize the TCO/p contact in a functioning TCO/p-i-n device using J-V measurements from a row of devices on a single isolated TCO strip. This method is useful for understanding resistance losses in modules and for diagnosing how plasma processing affects the TCO and junction properties since the TCO/p contact and TCO sheet resistance in a completed device structure are obtained. The method needs having a two adjacent TCO regions. The device is biased to possess standard current flow through its TCO/p contact region while the voltage is measured on the adjacent TCO pad which is electrically "floating". The second pad is thus a voltage sensing contact giving internal access to the potential in the biased device.

The purpose of this work is to determine the TCO/p contact and sheet resistances under light in a complete a-Si:H p-i-n solar cell device structure, which is very important for solar cell operation.

2. Experiment and analysis

The substrates were textured SnO_2-coated glass made by AFG (PVTCO). Single junction a-Si p-i-n layers were deposited by PECVD at BP Solarex. The SnO_2 strip of width W~0.8 cm had an In-solder contact to the SnO_2 at one end, and 6 devices (labeled m=1-6) fabricated in a row. Solar cell device areas were 0,27 cm^2. L is the distance along the TCO from the Ag contact to the m-th device, and L/W is the number of squares of TCO. Typically 2 rows of 6 devices were analyzed on each piece to establish repeatability.

Fig. 1 shows the experimental system used. Using a AM1.5 global simulator, the illuminated J-V characteristics were automatically measured by a software program. The only data needed for the analysis are measurements of the J-V characteristic from reverse bias to beyond open-circuit voltage (V_{OC}) in the light and in the dark at a given temperature.

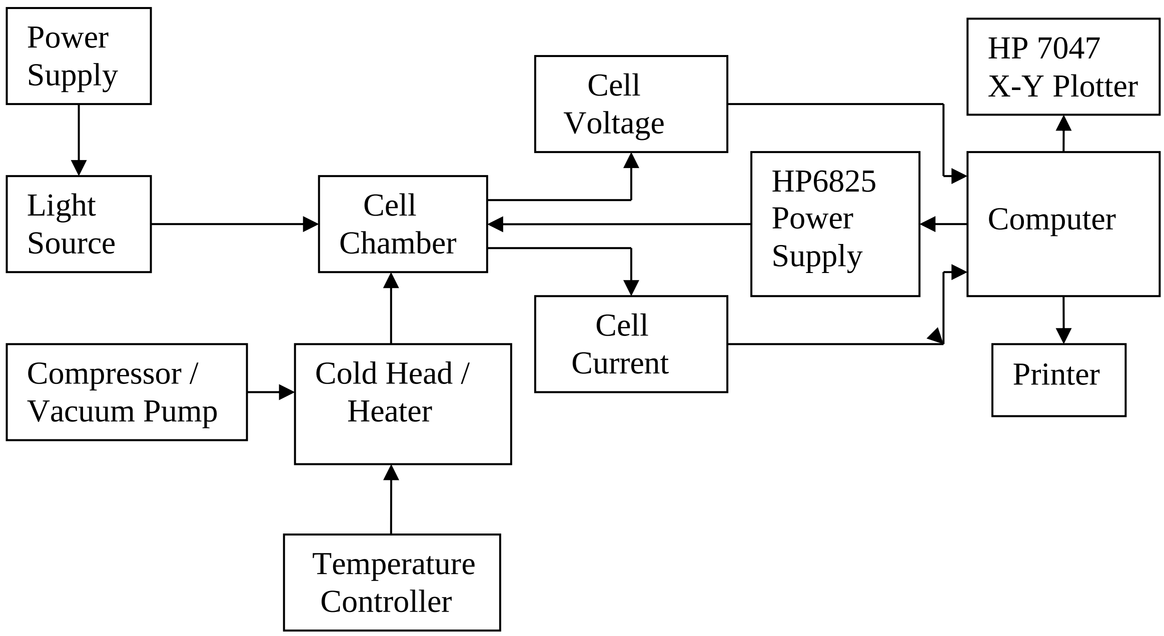

Fig. 1. Experimental set-up for measuring J-V characteristics.

Fig. 2 shows the side view of solar cell device structure which is glass/textured SnO_2/p (a-SiC)/i (a-Si)/n (a-Si)/metal. The top view of row of a-Si:H p-i-n devices (1-2-3) on scribed SnO_2 strips with contacts labeled A and B was shown in Fig. 3 for different external voltage connections (V_{1-A}, V_{1-B}, and V_{A-B}). The two SnO_2 strips of width W, with Ag-paste contacts labelled A and B, each have a row of square devices. The current in cells 1, 2, 3, etc., travels in the SnO_2, a distance L from each device to the SnO_2 contact A. The series resistance of the SnO_2 between the device and the contact is given by [14]

$$R_{TCO} = R_{SH} \text{ x } (L/W) \quad (1)$$

where R_{SH} is the sheet resistance of the TCO (SnO_2). As L increases, the series resistance of the TCO between the solar cell device and its SnO_2 contact increases. We assume that each device is identical, and its TCO/p contact is identical, this increase in R_{TCO} will be the only difference between devices in the same row.

As shown in Fig. 3, the three different measurement configurations (V_{1-A}, V_{1-B} and V_{A-B}) are to be characterized. For all three measurement conditions, it is biased such that the current flow is always between the cell's back contact (1) and the strip's TCO contact (A) as in a standard device J-V test. The difference between the 3 measurement cases is where the voltage (V) is mesured. In a standard J-V test measurement, the voltage V_{1-A} is measured between the same two contacts where the current (I) is flowing. This voltage V_{1-A} includes potential difference across the p-i-n junction structure, the TCO/p contact and potential difference dropped across the SnO_2 series resistance. If the voltage is measured across 1 and B or across A and B, there is no current passing through B so it is floating at the same potential as the p-layer contacting it, i.e., the p-layer over strip A. The SnO_2 strip B is used as a voltage terminal giving access to the internal voltage of devices on strip A. So, the voltage measured across device 1 and B ($V_{1\text{-}B}$) is only the potential difference across the p-i-n junction of a-Si:H solar cell device 1. This excludes the voltage dropped across TCO/p contact and TCO series resistance. Measuring the voltage across adjacent TCO strips ($V_{A\text{-}B}$) yields only the voltage dropped across TCO/p contact and TCO series resistance since strip B is floating at the same voltage as the p-layer above strip A.

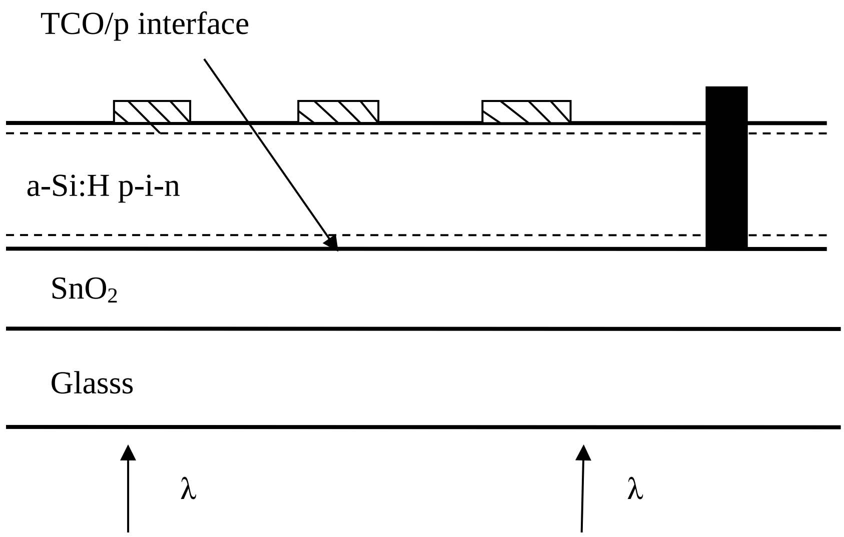

Fig. 2. Side view of row of a-Si:H p-i-n devices.

For the proposes of analyzing, we choose different J-V data by means of resistances. The three components of resistance and their relation to the three different voltage measurements are described in Eqs. (2-4). The three resistances which are dominated are the junction dynamic resistance R_J, the TCO/p contact resistance $R_{TCO/p}$, and the series resistance through the TCO R_{TCO}, as given in Eq. (1). The subscripts 1-A, 1-B, and A-B indicates voltage measured between contacts 1 and A, 1 and B or A and B as illustrated in Fig. 3 in detail. Here we assume that some other contact resistances, such as between the cell rear contact and the n-layer and between the SnO_2 and Ag contact, are ignorable. The resistances are defined in the the following [14]:

$$R_{1\text{-}A} = dV_{1\text{-}A}/dJ = R_J + R_{TCO/p} + R_{TCO} \quad (2)$$

$$R_{1\text{-}B} = dV_{1\text{-}B}/dJ = R_J \quad (3)$$

$$R_{A\text{-}B} = dV_{A\text{-}B}/dJ = R_{TCO/p} + R_{TCO} \quad (4)$$

$$R_J = dV/dJ = (AkT/q)/(J + J_{SC}) \quad (5)$$

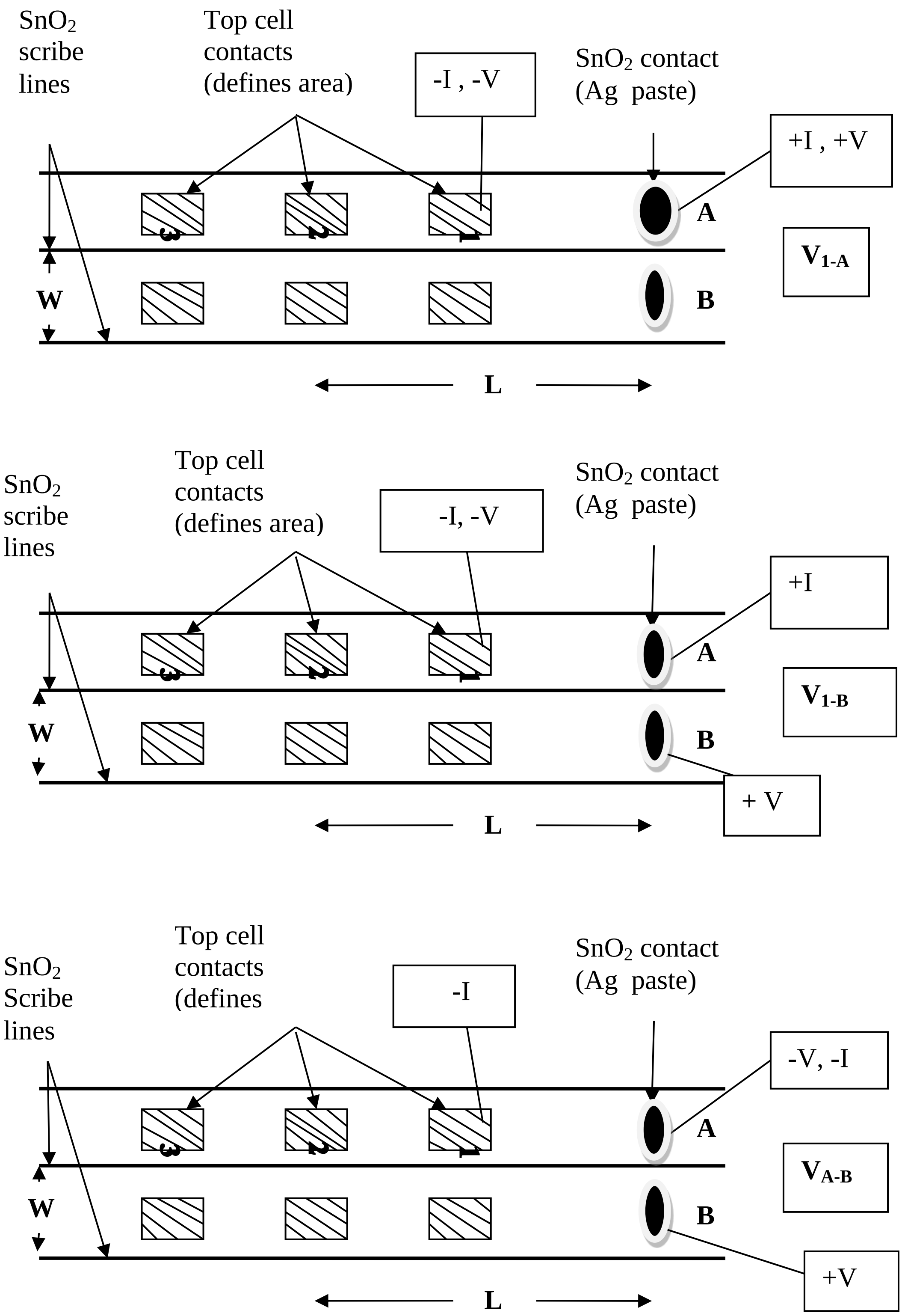

Fig. 3. Top view of row of a-Si:H p-i-n devices (1-2-3) on scribed SnO_2 strips with contacts labeled A and B. Current flow is established in p-i-n solar cell 1 between 1 and A while potential is measured between 1 and A, 1 and B, or A and B. SnO_2 strip B is floating at the same voltage as the p-layer over strip A.

Here the critical assumption is that TCO strip B is floating at the same voltage as the p-layer over strip A. If this is correct, Eqs. (2-4) predict that the difference in resistance between configurations 1-A and 1-B should be the same as that measured in configuration A-B. This resistance, R_{A-B}, must include the sum of the TCO/p contact and the TCO sheet resistance. From Eq. (1), the R_{A-B} vs L/W gives a straight line with a slope of R_{TCO} and an intercept of $R_{TCO/p}$. In this way, measuring all three resistances on a series of solar cell devices on the same strip with increasing L/W must allow determination of $R_{TCO/p}$ and R_{TCO}. For this reason, Eqs. (2-4) represent two independent method to recover R_{A-B}. This permits confirmation of the assumptions and measurements.

3. Results

Fig. 4 shows J-V characteristic curves for all three cases of voltage measurement on one cell (A9256-3C-S2 AFG) which was on AFG SnO_2. Standard solar cell J-V curves result when the V_{1-A} or V_{1-B} is measured while V_{A-B} gives a linear J-V curve through the origin. This linear J-V relation represents the TCO/p contact is ohmic according to Eq. (4). For the purpose of analysis, we obtain the values of resistances defined in Eqs. (2-4) at V_{OC}. So, for the configuration where V is measured across 1 and B, R_{OC} is dV_{1-B}/dJ at V_{OC}. Values of V_{OC}, FF and R_{OC} are recorded in Table 1. Note that the V_{OC} is the same between cases 1-A and 1-B, as expected since the p-i-n junction determines V_{OC}, but the FF increases in case 1-B since it excludes the TCO series resistance. The V_{OC} is zero in case V_{A-B} as expected from Eq. (4).

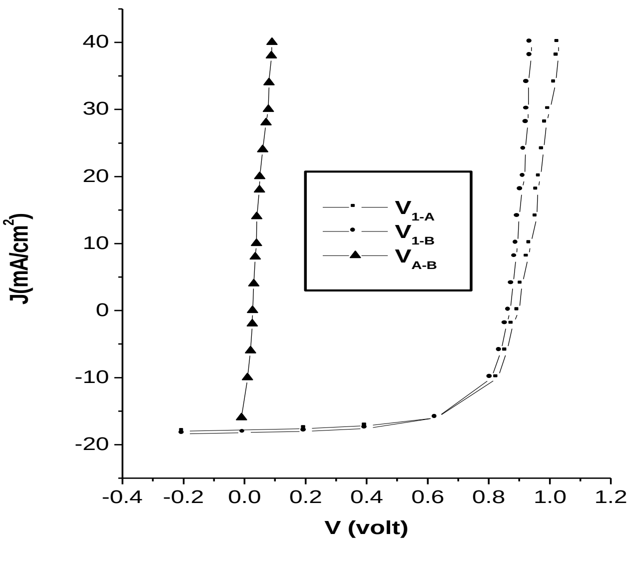

Fig. 4. J-V characteristics under illumination for a device (cell 1) with three voltage measurement cases. Parameters are given in Table 1.

Table 1. FF, resistance at V_{OC}, and V_{OC} for the three curves in Fig. 3 determined from three-voltage measurement cases on the same device under light.

Test voltage cases	FF (%)	R_{OC} (Ω . cm^2)	V_{OC} (V)
Cell 1 and A	68.3	4.74	0.89
Cell 1 and B	69.9	3.20	0.87
A and B	0	1.36	0

Fig. 5 illustrates a linear J-V behaviour for voltages measured across A-B for three devices on the same strip of TCO having different L/W ratios. Table 2 shows the values of resistance calculated from both methods. The both resistances increase with increasing L/W as expected, and the FF measured in standard case (V_{CELL-A}) decreases as L/W increases as predicted. Note the close aggreement in Table 2 between resistances obtained independently.

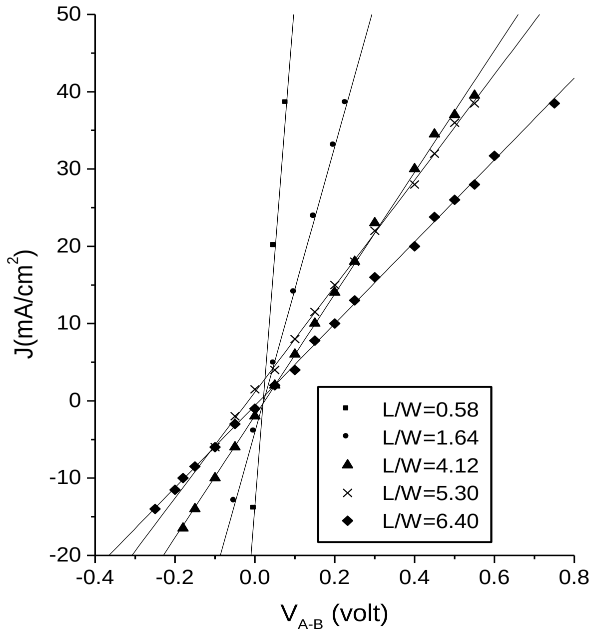

Fig. 5. J-V mesurements for five devices with varying L/W on the same TCO strip A. The potential was measured across the adjacent strips A and B.

Table 2. Resistance and FF for 5 devices with incresing L/W. $R(V_{A-B})$ obtained from slopes of lines in Fig.5. ΔR_{OC} obtained from difference of $R(V_{CELL-A})$ and $R(V_{CELL-B})$ at V_{OC} under light.

L/W	R (V_{A-B}) (Ω . cm^2)	ΔR_{OC} (Ω . cm^2)	FF (V_{CELL-A}) (%)
0.58	1.52	1.53	68.40
1.64	5.42	4.53	64.10
4.12	12.69	12.84	53.90
5.30	14.59	14.88	43.90
6.40	18.87	18.69	41.00

Fig. 6 indicates the two resistance (in Table 2) plotted against L/W for devices on the same strip of AFG SnO_2. ΔR_{OC} is the difference in R_{OC} for J-V measured as V_{CELL-A} and V_{CELL-B} while $R(V_{A-B})$ is the resistance determined directly from the slope of V_{A-B} as in Fig. 5. Obviously, they are also the same, verifying Eqs. (2-4) that the difference in resistance between $R(V_{CELL-A})$ and $R(V_{CELL-B})$ is the same as $R(V_{A-B})$, i.e., the TCO sheet resistance and TCO/p contact resistances. From the slope of line, R_{SH} is ~2.9 Ω/sq and from the intercept point, $R_{TCO/p}$ is ~0.2 Ω.cm^2. These values are smaller than those of dark results [16] as compared. This means that their roles in lost of efficiency are very small and negligable under illumination. Most of data for measuring R_{sh} and $R_{TCO/p}$ in the literature were taken in the dark, however our results represent them under light, and thus they give a good comparison.

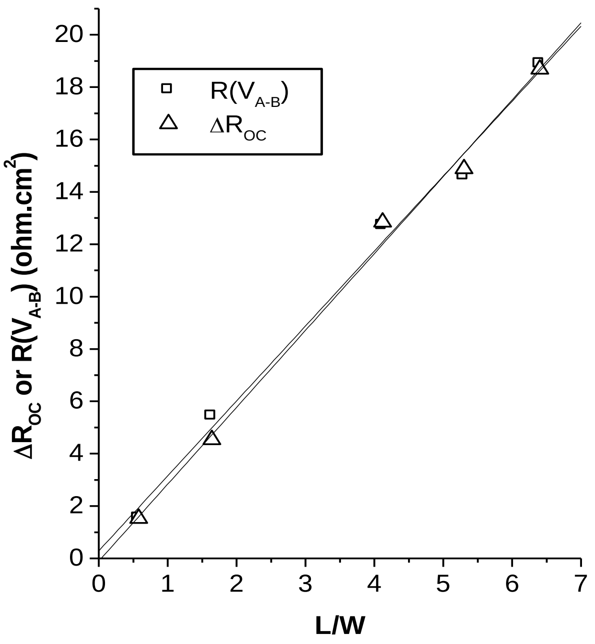

Fig. 6. Calculated resistance from both two methods vs L/W for row of cells on AFG SnO_2. The slope and intercept give the SnO_2 sheet resistance and TCO/p contact resistance respectively.

Fig. 7 shows dV/dJ as a function of 1/J for one device (L/W=0.60) in the dark and under illumination. It gives straight lines which are consistent with Eqs. (2-5). This result shows that the TCO/p contact is ohmic for both dark and light cases. It means that there is no blocking contact. However the slopes are different in the dark and light. Using Eq. (5), from the slopes of lines, we obtain A_{dark} = 1.8 and A_{light} = 0.3. The barrier height Φ, assumed to be activation energy E_a, of the TCO/p contact is determined as 56 meV from the temperature dependence of $R_{TCO/p}$ in the dark [16]. This value is smaller than 2kT, and thus not a rectifying barrier which means an ohmic contact. Unfortunately we could not determine and compare the barrier height under light due to some heating problems of light during measurements.

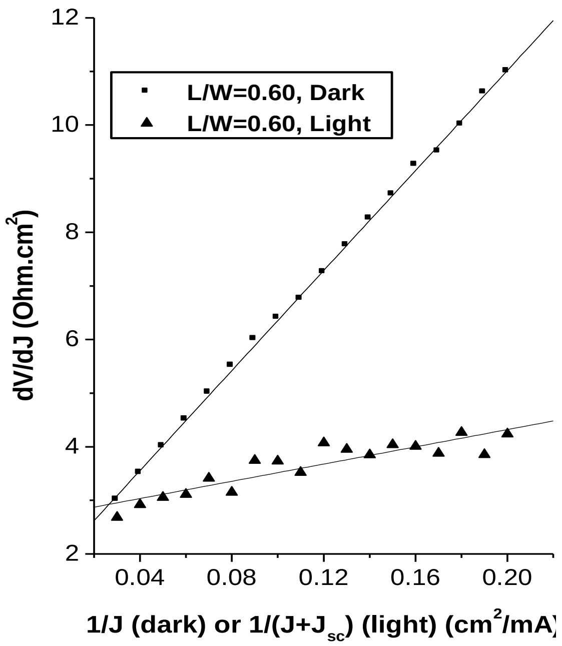

Fig. 7. dV/dJ versus 1/J or 1(J+J_{sc}) in the dark and under illumination respectively. The short-circuit current density, J_{sc} = 12.6 mA/cm^2, the open - circuit voltage, V_{OC} = 0.88 volt.

4. Conclusion

In conclusion, the TCO plays an important role in the thin film silicon solar cell structure and has a decisive influence on the efficiencies of a-Si:H p-i-n solar cells. As the conditions for the best values of several material parameters have to be found in a multidimensional deposition space, optimizing TCO for solar cells constitutes a very complex problem and deserves further research, including ideally a simultaneous up-scaling of the research results to industrially relevant substrate sizes.

Here we have used a different method to obtain TCO parameters in a device configuration under light. Solar cell devices should be deposited on scribed TCO regions. We have shown that the SnO_2/p contact indicates an ohmic contact. The TCO/p contact resistance is determined to be ~0.2 Ω.cm^2 and the sheet resistance 2.9 Ω/sq under illumination. These are smaller than those of dark results as compared. The A factor values of 1.8 and 0.3 were obtained at room temperature in the dark and under illumination respectively. Our results show a negligible loss in efficiency due to a very small TCO/p contact resistance under light.

Acknowledgments

We would like to thank Dr. S.S. Hegedus for using his laboratory and helpful discussions.

References

[1] T. M. Razykov, C. S. Frekides, D. Morel, E. Stefanakos, H. S. Ullal, H. M. Upadhyaya, Solar Energy **85**, 1580 (2011).

[2] N. Dwivedi, S. Kumar, S. Sing, H. K. Malik, Solar Energy **86**, 220 (2012).

[3] L. Ding, M. Boccard, G. Bugnon, M. Benkhaira, S. Nicolay, M. Despeisse, F. Meillaud, C. Ballif, Solar Energy Materials and Solar Cells **98**, 331 (2012).

[4] H. Hoppe, M. Seeland, M. Muhsin, Solar Energy Materials and Solar Cells **97**, 119 (2012).

[5] V. Jovanov, U. J. Plachoke, P. Magnus, H. Stiebig, D. Knipp, Solar Energy Materials and Solar Cells **110**, 49 (2013).

[6] E. V. Johnson, P. Prod'homme, C. Boniface, K. Huet, T. Emeraud, P. R. Caborrocas i, Solar Energy Materials and Solar Cells **95**, 2823 (2011).

[7] H. Zhu, J. Hüpkes, E. Bunte, J. Owen, S. M. Huang, Solar Energy Materials and Solar Cells **95**, 964 (2011).

[8] S. Fernandez, O. D. Abril, F. B. Naranjo, J. J. Gandia, Solar Energy Materials and Solar Cells **95**, 2281 (2011).

[9] A. M. K. Dagamseh, B. Vet, P. Sutta, M. Zeman, Solar Energy Materials and Solar Cells **94**, 2119 (2010).

[10] C. L. Tsai, C. L. Tsai, G. R. He, T. H. Su, C. F. You, Y. C. Lin, Solid-State Electronics **61**, 116 (2011).

[11] S. S. Hegedus, R. Kaplan, Progress in Photovoltaics: Research and Applications **10**, 257 (2002).

[12] J. Müller, B. Rech, J. Springer, M. Vanecek, Solar Energy **77**, 917 (2004).

[13] S. S. Hegedus, R. Kaplan, G. Ganguly, G. S. Wood, 28th IEEE Photovoltaics Specialist Conference, 2000, Anchorage, Alaska, pp. 728-731.

[14] S. S. Hegedus, M. Gibson, G. Ganguly, R. Arya, Material Research Society Symposium-Proceedings, **557**, 737 (1999).

[15] J. E. Phillips, R. W. Birkmire, B. E. McCandless, P. V. Meyers, W. N. Shafarman, Phys. Stat. Sol. (B) **194**, 31 (1996).

[16] R. Kaplan, B. Kaplan, Turkish Journal of Physics **26**, 459 (2002).

*Corresponding author: ruhikaplan@yahoo.com